



# Investigation of Dynamic Behavior of Stabilized Loose Sand by Microbially Induced Carbonate Precipitation

Hamid Nikouyeh<sup>a</sup>, Mohammad Azadi<sup>b,\*</sup>, Majid Ghayoomi<sup>c</sup>

<sup>a</sup> Department of Civil Engineering, Qazvin Branch, Islamic Azad University, Qazvin, Iran

<sup>b</sup> Department of Civil Engineering, Qazvin Branch, Islamic Azad University, Qazvin, Iran

<sup>c</sup> Department of Civil and Environmental Engineering, University of New Hampshire, Durham, NH, USA

Received: 19 May 2022; Received in revised form: 13 September 2022; Accepted: 22 October 2022

## ABSTRACT:

Due to the increasing number of construction projects, various methods, including more environmentally friendly methods, are used to increase the strength and bearing capacity of soil. Bio-cementation method is one of the newest methods that uses bacteria to form calcium carbonate crystals to make high-strength metamorphic products. This process can stabilize soil without breaking the original structure. One of these processes, which are common in nature, is the microbiological deposition of calcium carbonate by enzymatic hydrolysis of urea. Due to the size of soil grains and the size of bacteria used in sediment production, these bacteria will be able to produce sediment in silty, clay and sandy soils that form a wide range of soils. In this research, the effect of microbially induced carbonate precipitation (MICP) on the cyclic properties (liquefaction resistance, secant shear modulus and damping ratio) of loose sand is investigated via performing cyclic triaxial tests. Results revealed that carbonate precipitation could significantly increase the liquefaction resistance of Kuhin sand. So that the required cycles to reach the liquefaction criteria was increased from 6 for unstabilized sand to 97 (at cyclic stress ratio (CSR) of 0.2) for 4 times grouted carbonate precipitated sand. Also, this value was increased to 127 for 6 times grouted carbonate precipitated sand. Moreover, test findings show that CSR has an important effect on liquefaction resistance such that, the number of cycles leading to liquefaction decreased from 127 to 46 with the increase of CSR from 0.2 to 0.3 for 6 times grouted carbonate precipitated sand. Due to the carbonate precipitation, the secant shear modulus of sand increased by up to 67%, and also the damping ratio of sand increased by up to 50%.

## KEYWORDS:

Cyclic triaxial test, Liquefaction, Pore water pressure, MICP, Damping ratio, Shear modulus.

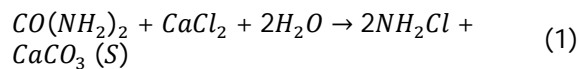
## 1. Introduction

In projects which based on geotechnical studies, the strength and bearing capacity improvement of ground are required, according to the existing conditions, various methods such as soil replacement, static and dynamic compaction, pile construction, reinforcement, injection of additives, and etc. are used to improve the soil (DeJong et al. 2006).

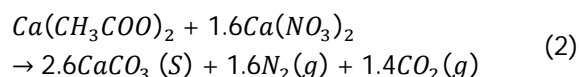
Bio-cementation method is one of the newest methods that uses bacteria to form calcium carbonate crystals to bind soil particles together without breaking the original structure. This method reduces permeability and has a low operating cost. It is also suitable in terms of environmental compatibility and a wide range of materials and microorganisms can be used in this method less harmful environmental consequences. One of these methods is to use bacteria in the soil to create bonds and adhesions between soil grains (DeJong et al. 2010). One of the most common

processes in nature is the microbiological calcium carbonate precipitation by enzymatic hydrolysis of urea. In nature, there are two processes for the in situ precipitation of calcite. In the first method, calcite is precipitated at saturated condition with calcium carbonate and under evaporation of the marine environment. This condition is more common in tropical regions. In the second method, calcite can be deposited by chemical reactions on grain surfaces, which is also the basis of soil microbiological improvement (Ozdogan, 2010). Numerous conditions such as physical, chemical, environmental, permeability, soil structure and composition affect the sedimentation and cementation process (Ismail et al. 2000). Due to the size of soil grains and the size of bacteria used in sediment production, these bacteria will be able to produce sediment in silty, clay and sandy soils (DeJong et al. 2010).

Bacteria that are used to strengthen and improve the soil must be able to discharge urease enzyme. These types of bacteria are divided into two categories: the first group is bacteria of the Bacillus family, which produce urease enzyme to catalyze the hydrolysis of urea and generate ammonium and calcium carbonate crystals (equation 1). The method in which these bacteria are used for sedimentation is called the biological calcium carbonate precipitation method (Harkes et al. 2010)



The second group is nitrogen-producing bacteria that release nitrogen gas during the reaction in the soil (equation 2) and, unlike the bacteria of the first method, are anaerobic and can precipitate in saturated soil conditions.



This method can increase the pH of the soil and provide the necessary conditions for calcite deposition. Unlike the biological calcium carbonate precipitation method, in which the oxidation of organic acids leads to the production of carbonate and there must be oxygen in the reaction medium, this method uses nitrogen-producing anaerobic bacteria and can be used in saturated soils. Also, in this method other cations can be used to replace and produce sediment (Van Paassen et al. 2010).

In this regard, to use the first group of bacteria in the biological calcium carbonate precipitation method, there are two methods to improve the soil: the first method, which is based on the biological stimulation of bacteria, by adding the required nutrients, activates the desired sediment-causing bacteria. In this method, bacteria are cultivated and grown in the soil. The use of this method is very

difficult due to many problems in providing a suitable culture medium, therefore, this method is mostly used to clean contaminated soils and is not very useful in improving engineering properties.

The second method is to increase the number of bacteria, in this method, the desired sediment-causing bacteria are added directly to the soil. In this method, all stages of culture and growth of bacteria are performed in the laboratory using special reactors (DeJong et al. 2010).

In this method, a special species of urease-positive bacteria (bacteria that have the ability to hydrolyze urea) that live in the soil and have alkaline-friendly properties cause a deposit in the soil by performing a hydrolysis reaction of urea. This reaction occurs in the presence of urea and calcium chloride in the soil and also raises the soil pH. The sediment formed from this reaction causes adhesion between the soil particles (Van Paassen, 2009).

## 2. Background

Feng and Montoya (2015) conducted a research on the effect of confining pressure and degree of cementation on the behavior of treated sand with microbial induced carbonate precipitation under drained condition. A series of drained triaxial compression tests were performed under different initial relative densities and confining pressures. As expected, dense specimens had higher strength, stiffness, and dilation than loose specimens. With increasing effective confining pressure, the strength increased, and the behavior of volumetric deformation changed from dilated to contractile.

Han et al. (2016) performed research on the liquefiable sands improved by microbially induced carbonate precipitation using cyclic triaxial tests. They also compared this used improvement method with the chemical improvement method of silica gel. The results of the experiments showed that the improvement of sands with one to two times of use of bacterial and salt solution has a great effect on reducing the pore water pressure and axial strain in cyclic loading. Comparison of two different used methods showed that the strength of improved samples with two methods is almost same. However, the sample improved by method of MICP takes only two days to reach the desired strength, while the sample improved by silica gel method will take between 4 to 56 days to achieve the same strength.

Darby et al. (2019) conducted 80 g centrifuge shake table tests on three different sets of treatment models with CaCO<sub>3</sub> contents of 0.8%, 1.4%, and 2.2%; the results showed that, after MICP treatment, the cone penetration resistance of the sand increased from 2 MPa to 5, 10, and 18 MPa and that the shear wave velocity increased from 140 m/s to 200, 325, and 660 m/s. As the level of

cementation increased, the liquefaction resistance increased, no further liquefaction occurred, and the mechanical properties of the model sample gradually changed from those of soil to those of rock.

Lin et al. (2020) studied the effect of microbially induced carbonate precipitation (MICP) on stiffness and permeability of sands. Also, they investigated the effects of  $\text{CaCO}_3$  distributions on the mentioned parameters. Based on their results it was determined that the dominant  $\text{CaCO}_3$  distributions were a combination of grain-coating and matrix-supporting.

Zhang et al. (2020) performed several shake table tests to evaluate the seismic performance of MICP-treated calcareous sandy foundations. They showed that the strength and stiffness of the model were considerably improved and during the shaking, the excess pore pressure ratio and surface settlement of MICP-treated model were significantly decreased. Also, the test results indicate that use of the MICP method can significantly improve the strength, stiffness and liquefaction resistance of calcareous sand.

Most of the previous studies on MICP-treated sands have focused on mechanical properties and permeability characteristics under static loading even though information on the impact of MICP on liquefaction potential of sand under dynamic loading and dynamic aspects of MICP-treated sand at low strains, such as small-strain dynamic shear modulus and damping ratio, is limited.

Therefore, this study aims at providing technical data on the cyclic triaxial behavior of sand treated with MICP. In particular, the effect of the number of cementation solution grouting on liquefaction potential, PWP generation, variation of shear modulus and damping ratio of samples was investigated by using cyclic triaxial tests.

### 3. Experimental program

#### 3.1. Materials

##### 3.1.1. Kuhin sand

The experiments are carried out on poorly graded sand with specific gravity of 2.64 (based on ASTM D854-14) and the maximum and minimum void ratios of 0.86 (corresponding to  $\gamma_{\text{min}}=1.54\text{g/cm}^3$ , based on ASTM D4254-16) and 0.45 (corresponding to  $\gamma_{\text{max}}=1.81\text{g/cm}^3$ , based on ASTM D4253-16) respectively, that was provided from the Kuhin in the Qazvin in Iran. Based on the Unified Soil Classification System, the soil was marked as poorly graded sand (SP), ASTM D2487-17. Also, its mean grain size (D50) was determined 0.24mm. Furthermore, the curvature and uniformity coefficients were 1.03 and 1.73, respectively. Fig. 1 shows the grain size

distribution curve of Kuhin sand, which was determined according to ASTM D422-63.

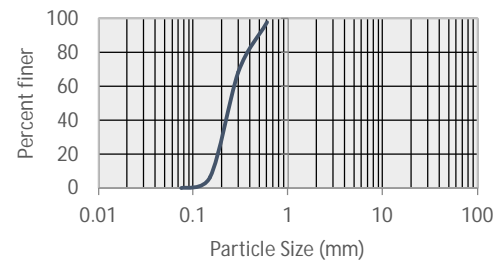


Fig. 1. Grain size distribution of Kuhin sand

#### 3.1.2. Bacterial characteristics and injection method

The bacterium used in this study belongs to the Bacillus family with the scientific name of *Sporosarcina pasteurii*. The bacterium was prepared from the collection center of fungi and industrial bacteria of Iran under number PTCC 1645 (DSM33) in lyophilized form.

Since the used bacteria was lyophilized and powdered, the bacteria were activated before the experiments. For this purpose, the powder was cultured in nutrient broth medium according to the instructions on the box.

According to the results of previous research, the selected culture medium to prepare the biomass of this bacterium, the liquid medium consisting of nutrient broth and urea were 8g/l and 20g/l, respectively in a 0.13M Tris Buffer with pH=9.0. After preparing this medium, the Erlenmeyer flask was closed using cotton and aluminum foil to remain sterile and prevent the penetration of any germs into it and was placed in an autoclave for 15 minutes at a temperature of 121°C. After the culture medium was equilibrated with the laboratory temperature, the culture medium was stored at 4°C in the refrigerator until the time of use. To prepare the bacterial suspension for use in soil experiments, at first 50ml of the above culture medium was added to the solid culture of bacteria in Erlenmeyer 500 ml, at a temperature of 30°C with a rotation speed of 170 rpm in a shaker incubator overnight. From the mentioned overnight culture under sterile conditions and with the aid of microbial hood, the amount of 1 ml per 100ml of new medium was transferred to 1000ml Erlenmeyer containing 300 ml of the same culture medium. This Erlenmeyer was then placed inside a shaker at laboratory temperature at a vibration rate of 170rpm. Based on the growth curves obtained in previous research, the resulting medium after 24 to 48 hours of bacterial culture, was at the end of the exponential growth phase and the beginning of the dormant phase, and at this stage the concentration

active bacterial in the culture medium reaches the maximum possible amount according Whiffin (2004). Therefore, the desired culture medium is removed from the shaker and is harvested to extract bacterial cells (bacterial biomass).

To harvest the culture medium, 220ml of the culture medium containing bacteria was poured into 8 centrifuge tubes and was placed in a centrifuge for 10 minutes at 4000rpm to separate the bacterial mass from the culture medium. After this step, the clear solution of the upper part of each tube, which is empty of bacteria, was discarded and the solid mass of bacteria that remained in the bottom of the tube was suspended by 0.9% NaCl solution. This suspension was used to prepare different concentrations used for cyclic tests.

To prepare different concentrations used in the experiments using a spectrophotometer, the amount of light absorption ( $OD_{600}$ ) of the suspension was read. For this purpose, 0.9% NaCl solution was used as a control sample and also as a solution used to dilute the suspension (if necessary). After adjusting the concentration or light absorption of the bacterial suspension ( $OD_{600}$ ), the amount of urease activity of the prepared suspension was measured (1.1-1.9mM urea/min). The  $OD_{600}$  of this mixture was between 0.8 and 1.2. Then the container containing the suspension was closed with cotton and placed in a refrigerator at 4 ° C. In order to equalization of the test conditions and reduce the test errors, the bacterial suspensions used in the experiments of this study were kept for 24 hours at a temperature of 4 ° C and away from nutrient.

Prior to injection, the sample is rinsed with deionized distilled water to the extent of the sample volume (Whiffin et al. 2007; Lin et al. 2016). After the washing phase, the bacterial suspension is first injected into the soil by gravity injection (due to the shallow depth of the samples, this type of injection was used). After this step (stabilization phase) and after 6 hours, cementation solution such as urea and calcium chloride with a concentration of 0.5M are combined and poured on the soil. The sample is then cured at laboratory temperature for hydrolysis of urea and produce calcite. Depending on the need, a cementation solution containing urea and calcium chloride is added to the soil 4 or 6 times. Figures 2-3 show different phases of this procedure.

### 3.2. Sample preparation

For preparing samples in laboratory different methods including wet/moist tamping, air pluviation, wet pluviation, water sedimentation and under compaction can be used. In this research, air pluviation method is used for sample preparation. Cylindrical samples with a diameter of

70mm and a height of 140mm are prepared for the cyclic tests.

The PVC mold with two semi-cylinder parts used to prepare the samples. In order to prevent soil grains from ran out from beneath of the mold and filtering, galvanized mesh was used in the bottom of the mold and also a circular plate made of Plexiglas with 5 holes was used to control the discharge of the injected material. The injection procedure of microbially induced carbonate precipitation into the prepared samples was explained in the previous section.



Fig. 2. cementation solution of 0.5 M urea and 0.5 M calcium chloride



Fig. 3. Injection of cementation solution into soil samples by gravity method

### 3.3. Test equipment and procedure

Cyclic triaxial tests were conducted on unstabilized and stabilized samples based on ASTM D3999 and ASTM D5311 to assess the impact of stabilization on the liquefaction resistance and dynamic characteristics, including damping ratio and secant shear modulus.

In this research, an automated triaxial test device was used (AG Geoinstrument). The overall view of cyclic triaxial apparatus is presented in Fig. 4. This apparatus consists of four parts: a board, a loading frame, a cell, and other device accessories.

The board is used to display and control the applied loads inside and outside the sample during saturation, consolidation, and loading phases. Two onboard gauges are also included to visually observe the pressure and suction values. In addition, three graduated burettes are included on the board in order to monitor the Top Back Pressure (TBP) and Bottom Back Pressure (BBP) to provide the required water. By using these burettes, the amount of input and output water of the sample are determined. Furthermore, to

control the amount of input and output water, two valves are also installed on the board. Besides, electrical sensors for capturing the water pressure and controlling the valve to set the cell pressure are provided as well. The range over which the sensors can precisely work is from zero to 1000kPa (Noorzad and Amini, 2014).

The loading frame applies the loading on a sample. This part of the apparatus includes a base, two columns, a beam, and a loading jack. To control and observe the data, three electrical parts including a server valve, a load cell, and a displacement sensor are installed on the loading frame. The capacity of the load cell used in this study is up to 500 kg, and the displacement limit for the sensor is 50 mm. The sample is placed in a cell, which can bear the pressure up to 850kPa. There are four valves below the cell, each of which has a specific function: one is for applying the cell pressure, one is for applying the top back pressure, and the other two are for applying the bottom back pressure or drainage. In addition, the controlling system includes the sensors, operators, a data logger, and processing software.

In this research, 34 cyclic triaxial tests were performed on Kuhin sand and treated samples (Table 1). After the sample was reached the desired curing time, it was assembled in the cyclic triaxial cell, and the specimen was flushed with carbon dioxide at low pressure for at least one hour to eliminate entrapped air. Next, the sample was flushed with using de-aired water until the total volume of the water was at least equal to about twice the primary volume of the specimen until saturation (Noorzad and Amini, 2014). Subsequently, cell pressure and back pressure were increased step by step with sufficient time between increments to enable equalization of water pore pressure throughout the sample.

The sample saturation was continued until the B value reaches to 0.95 or higher (Banerjee et al. 2018). To consolidate the samples isotropically, the cell pressure was increased at a constant back pressure of 300kPa, till the difference between cell and back pressure became equal to a wanted effective confining pressure ( $\sigma_3$ ), which was selected as 100, 200 and 300kPa in this study.

Then, a sinusoidal stress with 0.5 HZ frequency was applied to the consolidated specimen, during undrained condition, and the axial load, vertical displacement, and PWP were logged with increment of 0.001 sec. A cyclic stress ratio ( $CSR=q_{cyc}/2\sigma_3$ ) from 0.15 to 0.3 were used to simulate medium and severe earthquakes that are relevant for the studied region. The liquefaction is specified in this research, as the condition where the double amplitude of axial strain (DAAS) over cyclic loading reaches 5% (Keramatikerman et al. 2017).

**Table 1.** Test condition of each sample in undrained cyclic triaxial test (L=liquefaction potential, G-D= shear modulus and damping ratio, samples with \* is untreated)

sample	Conf. stress (kPa)	Test	sample	Conf. stress (kPa)	Test	sample	Conf. stress (kPa)	Test
Sand1*	100	L	Biocyc1	100	G-D	Biocyc16	100	G-D
Sand2*	200	L	Biocyc2	100	G-D	Biocyc17	200	G-D
Sand3*	300	L	Biocyc3	300	G-D	Biocyc18	300	G-D
Sand-G1*	100	G-D	Biocyc4	300	G-D	Biocyc27	200	G-D
Sand-G2*	200	G-D	Biocyc5	200	G-D	Biocyc28	100	G-D
Sand-G3*	300	G-D	Biocyc8	200	G-D	Biocyc29	200	G-D
Sta-4-1	100	L	Biocyc9	100	G-D	Biocyc30	300	G-D
Sta-4-2	200	L	Biocyc10	200	G-D	Biocyc31	100	G-D
Sta-4-3	300	L	Biocyc11	300	G-D	Biocyc32	200	G-D
Sta-6-1	100	L	Biocyc12	100	G-D	Biocyc33	300	G-D
Sta-6-2	200	L	Biocyc13	200	G-D			
Sta-6-3	300	L	Biocyc15	300	G-D			



**Fig. 4.** Cyclic triaxial device and its accessories

To calculate the damping ratio and secant shear modulus, it is necessary to determine the stress-strain response of the soil, demonstrating the resulting hysteresis loops. Since deviator stress and axial strain are measured in the cyclic triaxial tests, to calculate the damping ratio and secant shear modulus, hysteresis loops must be plotted in terms of shear strain and shear stress. The relationship between the above parameters is as follows (Kokusho, 1980):

$$\Delta\tau = \Delta\sigma / 2 \quad (3)$$

$$\Delta\gamma = (1 + \nu)\Delta\varepsilon \quad (4)$$

Where  $\Delta\tau$  is the variation of shear stress,  $\Delta\sigma$  is variation of axial stress,  $\Delta\gamma$  represents variation of shear strain,  $\nu$  is the Poisson's ratio, and  $\Delta\varepsilon$  is the variation of axial strain. Under undrained conditions for a fully saturated clayey soil, the value of  $\nu$  can be taken as 0.5. Hysteresis loops are obtained by plotting a shear stress-strain curve,

which can then be utilized to calculate the shear modulus ( $G$ ) and the equivalent damping ratio ( $D$ ) (Kokusho, 1980).

Also, to measurement of calcite precipitation of bio-cemented samples was measured post-failure by acid washing. Each sample was split into four pieces. The pieces were then dried at 105°C for about 24h and their weights were recorded before hydrochloric acid (0.5M) was added. Each piece was then washed with tap water while making sure that no soil particles were lost in the process. The pieces were dried again for about 24h and their weights were measured. The gaps in weight, before and after the addition of hydrochloric acid, were calculated to be the quantities of precipitated calcite (Table 2).

**Table 2.** Specification and results of the conducted cyclic triaxial tests

sample	CSR	N	DAAS (%)	$r_u$	CaCO <sub>3</sub> (%)	$D_r$ (%)
Sand	0.15	12	>5	>1	0	39.1
	0.18	8	>5	>1	0	39.1
	0.2	6	>5	>1	0	39.1
Sta-4 grouting	0.2	97	>5	>1	1.2	42.6
	0.25	56	>5	>1	1.06	41.8
	0.3	35	>5	>1	1.43	44.1
Sta-6 grouting	0.2	127	>5	>1	2.21	45.6
	0.25	77	>5	>1	2.24	47.5
	0.3	46	>5	>1	2.10	45.7

#### 4. Results and discussion

The timeline of axial strain, the ratio of excess pore water pressure, and the applied deviator stress, for unstabilized sand with at CSR values of 0.2 and 0.15 are shown in Fig. 5-6, respectively. It is observed from the Fig. 5 (a) and 6 (a) that applying constant cyclic deviator stress increased the axial strain gradually, until the DAAS of 5% (liquefaction criterion) was reached. The ratio of excess water pore pressure that was specified as the ratio of developed excess pore water pressure to the confining stress ( $r_u = \Delta U / \sigma'_3$ ) (Keramatikerman et al. 2017), increased gradually with time. Fig. 5(C) and 6(C) show the development of  $r_u$  for these two samples. As it is observed, the generated  $r_u$  within the specimen periodically changed during cyclic loading, while its value increased in each loading cycle in a cumulative manner. As can be seen, the specimens with lower CSR reached initial liquefaction ( $r_u=1$ ) before failure, while for the specimen with a higher CSR, the initial liquefaction and failure occurred at the same time. More details on this are provided below.

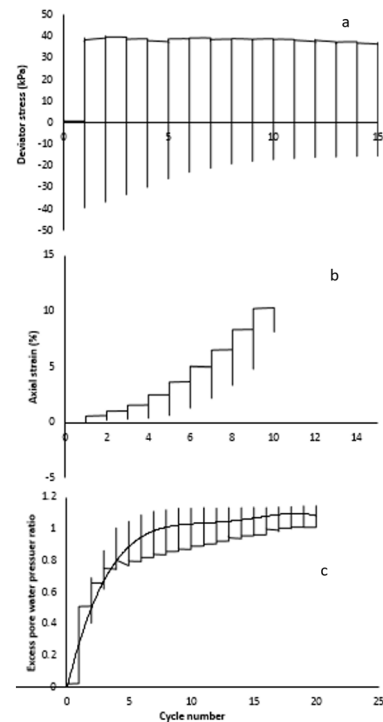


**Fig. 5.** Timeline of: a) deviator stress, b) axial strain, c) excess pore water pressure for unstabilized sand (CSR=0.2, and  $\sigma_3=100\text{kPa}$ )

#### 4.1. Liquefaction resistance

The triaxial testing program of this study is shown in Table 2, which shows the test results in terms of the ratio of developed pore water pressure at the end of the experiment, the number of applied cycles to reach the liquefaction, the range of double amplitude axial strain, percentage of carbonate precipitation (CaCO<sub>3</sub>) and relative density of the sample. As previously noted, the liquefaction criterion was considered as the achievement of the double amplitude axial strain to 5%. According to Table. 2 it is clear that with the stabilization via MICP method, relative density ( $D_r$ ) of the sand was increased slightly and with increasing the number of cementation solution grouting, the amount of  $D_r$  increase has also increased. Moreover, Table 2 shows that MICP-treated sand needs more cycles to reach the liquefaction. At the same CSR (CSR of 0.3), with increasing the number of cementation solution grouting (from 4 grouting to 6 grouting), the required cycles to reach the liquefaction also increased (from 35 to 46). These results showed that due to the MICP-treatment the liquefaction resistance of the sand was improved. This can be ascribed to the cementation of precipitated calcite.

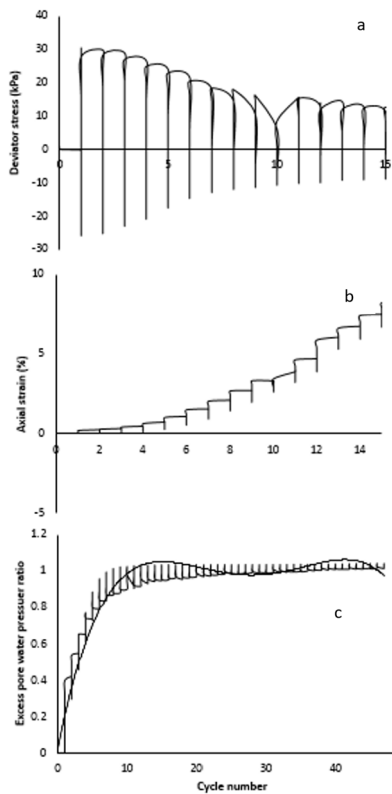


**Fig. 6.** Timeline of: a) deviator stress, b) axial strain, c) excess pore water pressure for unstabilized sand (CSR=0.15, and  $\sigma_3=100\text{kPa}$ )

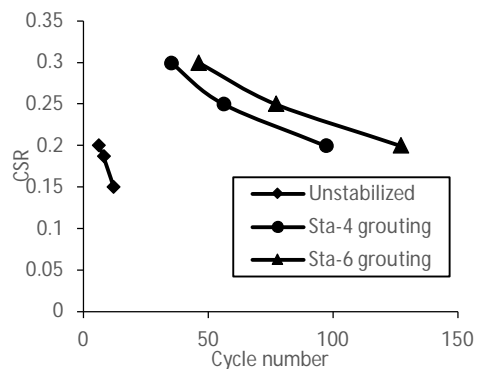


**Fig. 7.** Comparison of cyclic resistance for untreated and MICP-treated sand

Fig. 7 shows the cyclic resistance of untreated and MICP-treated sand. As stated before, also it can be concluded from this figure that soil treatment (with MICP) had a considerable effect in decreasing the liquefaction potential (or increase of cyclic resistance). For example, the number of cycles leading to liquefaction at CSR of 0.2 is changed from 6 for the untreated sand to 97 for the MICP-treated sand with 4 times cementation solution grouting at 100kPa confining pressure. The corresponding value for the MICP-treated sand with 6 times cementation solution grouting was 127 cycles. Actually, the resistance of treated sand against liquefaction increased with increasing calcite

precipitation, which was in consistent with the behavior observed by previous researchers (Simatupang et al. 2018).

Fig. 8 shows the developed axial strain for untreated and MICP-treated sand with different injection frequencies at 100kPa confining pressure and CSR of 0.2. As it can be seen, untreated sand exhibited a sudden growth in axial strain, and reached a DAAS of 5% (liquefaction criterion) in fewer cycles (6 cycles); however, for the treated sand, increase in axial strain against applied cyclic loading is low at the beginning cycles and occurred gradually at the last cycles. This behavior was more noticeable with a growth in the calcite precipitation.

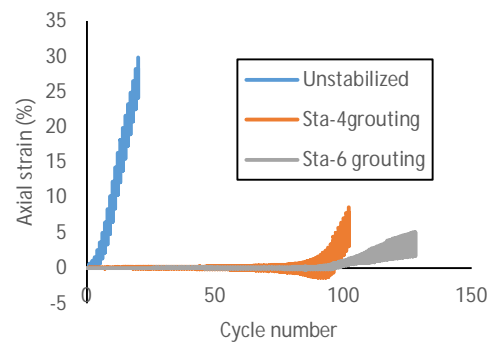


**Fig. 8.** Comparison of developed axial strain for untreated and MICP-treated sand at confining pressure of 100kPa and CSR of 0.2

The development of excess PWP ratio ( $r_u$ ) for untreated and treated (calcite precipitation with both two injection frequencies) sand at confining pressure (CP) of 100kPa and CSR value of 0.2 is shown in Fig. 9. As it can be observed from the figure, the rate of PWP development in the untreated sand is rapid and the initial liquefaction state ( $r_u=1$ ) occurs in fewer cycles of applied cyclic loading, while in the treated sand (with both two injection frequencies), this rate is significantly reduced and the initial liquefaction state is reached in more cycles. Actually, it can be stated that the precipitation of calcite in the sand delays its initial liquefaction state due to the cementation of precipitated calcite, which this cementation confines the particle movements and cause to a decrement in PWP throughout the specimen. Another point that can be concluded from this figure and Fig. 8 is that excess PWP in the treated sand increased gradually and more cycle is needed to reach the initial liquefaction, and also the initial liquefaction state didn't coincide with the failure.

Generally, the improvement of liquefaction resistance of calcite precipitated sand can be explained as below. Calcite binds the particles of sand. In comparison to the untreated sand, the behavior of treated sand is stiffer and the developed excess PWP remains low, especially at the beginning cycles of applied loading. This is

attributed to the created bonds between the sand particles due to the precipitated calcite. Actually, this agent stabilizes the skeleton of the soil. However, as shown in Fig. 8, when the number of loading cycles increases and the axial strain exceeds about 0.5%, the effect of precipitated calcite decreases, and the axial strain amplitude starts to increase in a larger ratio almost the same as the untreated one. Simatupang et al. (2018) and Lin et al. (2020) performed triaxial compression tests on the untreated and calcite-treated sand and reported the same results. They observed that the response of calcite-treated sand was very similar to that of untreated one for axial strains above the 0.25 and 0.5%. The percentage of calcite contents in their samples were equal to 0.9-2.5%, which is almost similar to the percentage used in this study (1.06-2.24%).

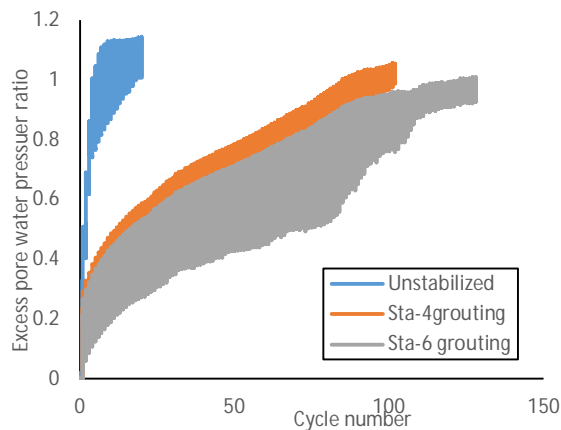


**Fig. 9.** Comparison of developed excess pore water pressure ratio for untreated and MICP-treated sand at confining pressure of 100kPa and CSR of 0.2

The effect of the applied CSR on changes of the developed excess PWP ratio in untreated and treated samples is evident in Fig. 10. By increasing the applied CSR, due to the increase of the applied cyclic stress to the sample, more excess PWP was developed because of increase in the created axial strain in the sample and led to the achievement of both untreated and treated samples to liquefaction conditions (the double amplitude axial strain is reached to 5%). Similar observations have been made in this issue for some soils (Guo et al. 2013, Chen et al. 2016).

As mentioned earlier, the trend of changes of excess PWP ratio in the untreated sample is accompanied by a rapid increase in the initial cycles. With increase of CSR, the speed of this increase has also increased, and the sample has reached to the initial liquefaction ( $r_u=1$ ) in a smaller number of cycles (has reduced from 12 to 6 cycles). For the treated sample, the trend of changes of excess PWP ratio is gradual with the increase of cycle numbers. Also, in this case, increasing the CSR value has increased the rate of

increase of excess PWP ratio so that the sample in this case has reached to the initial liquefaction ( $r_u=1$ ) in 46 cycles.

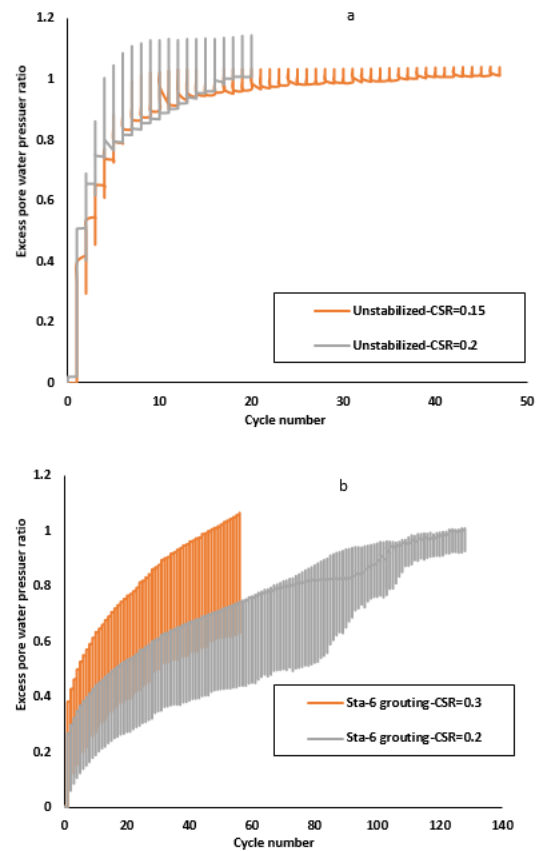


**Fig. 10.** The effect of CSR on changes in excess pore water pressure ratio for: a) untreated sand, b) treated sand

Stress-strain curves (hysteresis loops) for untreated and MICP-treated samples with injection frequencies of 6 are shown at different CSRs (0.15-0.3) in Fig. 11. It is evident from this figure that due to treatment, the developed axial strain in the sample (the size of the formed hysteresis loops) is reduced. In other words, due to the application of the same loading cycles at a CSR of 0.2, the stabilized samples undergo less deformation. Additionally, according to the results shown in Fig. 11, the effect of treatment on the CSR of 0.3 is qualitatively similar to that of the CSR of 0.2. Contrary to the untreated sample which double amplitude axial strain reaches faster to five percent, in the treated sample, the strain increases gradually at a slower rate.

Generally, it can be stated that MICP-treated samples demonstrated an inelastic behavior and the mean slope of the loops decreased from cycle to cycle, which is indicating stiffness degradation of these samples over cyclic loading.

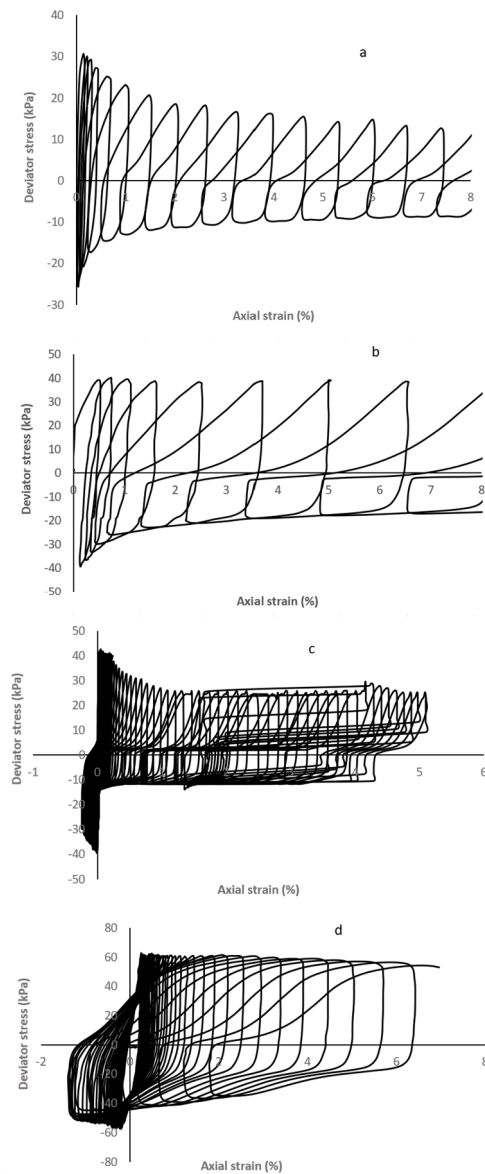


**Fig. 11.** Stress-strain curves for: a) untreated, CSR=0.15, b) untreated, CSR=0.2, c) MICP-treated, 6grouting, CSR=0.2, d) MICP-treated, 6grouting, CSR=0.3

## 4.2. Cyclic properties

### 4.2.1. Shear modulus

Shear modulus was calculated based on obtained hysteresis loops and according to ASTM D3999. Fig. 12 shows the effect of MICP-treatment on the variations of shear modulus of the soil at confining pressure of 100kPa. The soil shear modulus increased due to MICP-treatment up to 67%. As stated earlier, MICP-treatment leads to aggregation of soil structure and binding the soil particles. As an outcome of this phenomenon, particle deformation is decreased and thus the shear stiffness of the soil is increased. Increasing the number of loading cycles leads to more shear strain creation and consequently more

development of pore water pressure. So, the stiffness of the sample decreases. This is the reason of shear modulus reduction for both untreated and MICP-treated samples as a result of an increase in the shear strain (Fahoum et al. 1996, Hoyos et al. 2004).

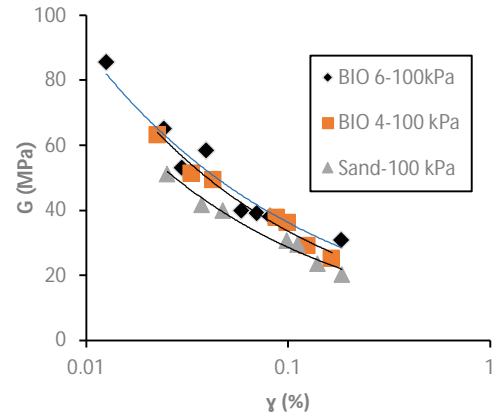


**Fig. 12.** Effect of MICP-treatment on the shear modulus variation of sand

In other words, it can be stated that by exposing the completely saturated soils to cyclic loading in undrained conditions with intensities that produce a medium or large shear strain (similar to the strains created in this study), soil particles irreversibly move towards each other. As a result, the soil structure changes permanently, its strength and stiffness decreases, and the excess pore water pressure continuously changes with the cycle numbers.

The effect of confining pressure on the variations of shear modulus of MICP-treated sand is shown in Fig. 13. The figure shows that the shear modulus has increased with increasing confining pressure. So that by increasing confining pressure from 100 to 200kPa, the shear modulus has increased by about 57%. For a confining pressure of 300kPa, the increment rate is about 93%. The reason for this can be attributed to the fact that the created bonds (due to calcite precipitation) between the sand particles are supported by the confining pressure. Similar trends were reported for the bonding strength of cement stabilized and lignosulfonate stabilized samples by Athukorala (2013) and Ta'negonbadi and Noorzad (2018). Moreover, with increasing confining pressure, the confinement of soil structure increases and the deformation of particles due to cyclic loads decreases, which also increases the shear stiffness of the soil.

### 4.2.1. Damping ratio

Fig. 14 shows the effect of MICP-treatment on variations of soil damping ratio at confining pressure of 100kPa. As seen from this figure, due to

treatment, the damping ratio of the soil increased. Since the damping ratio increases with increase of soil deformation (Wang et al. 2012) and, as stated in shear modulus section, the deformation in the soil due to MICP-treatment has decreased and the shear modulus increased.

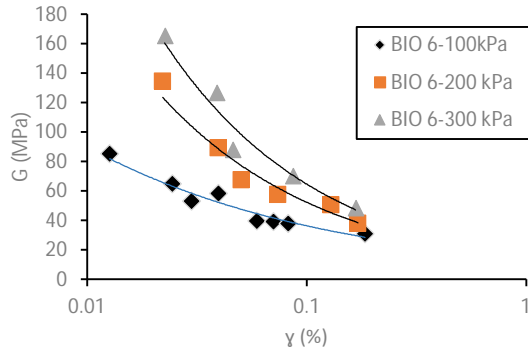


**Fig. 13.** Effect of confining pressure on the variations of shear modulus of MICP-treated sand

In fact, due to MICP-treatment, soil deformations (elastic deformations) are reduced and most of these deformations that occur due to cyclic loading are plastic deformations (Poulos 1988). Festugato et al. (2021) concluded the same result for deformations of the cement stabilized sand. Damping is also the result of the occurrence of plastic deformations in the soil structure (Poulos 1988). In the untreated sample, the major occurred deformations are elastic, so the amount of damping in this case is low. As can be seen from Fig. 14, the damping ratio increased with increasing the number of cementation solution grouting. According to the above, with increasing the number of cementation solution grouting, increasing stiffness and limiting deformation occurs, but the rate of increment in deformation also increases in this case, which increases damping ratio up to 50%. The same result is reported for the cement stabilized sand by Festugato et al. (2021).

Furthermore, it is evident from Fig. 14 that by increasing the cycles of applied loading (increase of shear strain), the damping ratio has increased for both untreated and MICP-treated samples. The reason for this increase can be attributed to the fact that by increasing the shear strain and the progress of the dynamic strain, soil specimens regularly loosen under the effect of shear stress. The rubbing effect increases, which consumes further energy. As a result, the damping ratio increases by the increase of the dynamic strain as a result of the increment of shear strain (Wang et al. 2012).

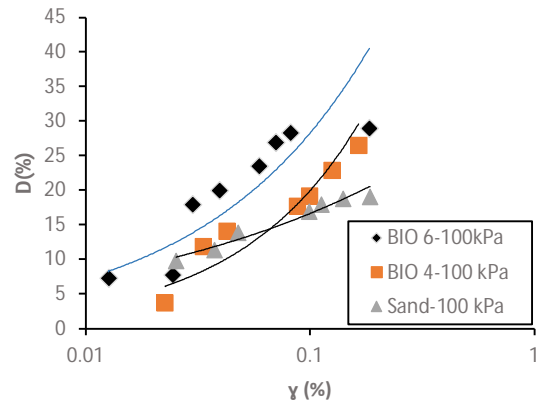


**Fig. 14.** Effect of MICP-treatment on the damping ratio variation of sand

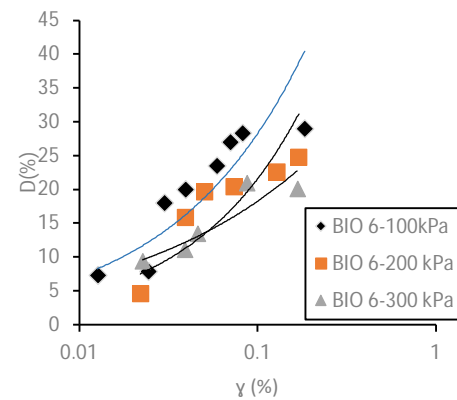


**Fig. 15.** Effect of confining pressure on the variations of damping ratio of MICP-treated sand

The effect of confining pressure on the variations of damping ratio of MICP-treated sand is shown in Fig. 15. The figure shows that the damping ratio has decreased with increasing confining pressure. So that by increasing confining pressure from 100 to 200kPa, the damping ratio has decreased by about 15%. For a confining pressure of 300kPa, the decrement rate is about 28%. The reason for this can be attributed to the fact that with increasing confining pressure, the confinement of soil structure increases and the deformation of particles due to cyclic loads decreases, hence the damping ratio of the soil decreases.

#### 4.3. Effect on microstructure

The SEM and EDS images were used to better understand the impact of MICP-treatment, and to identify the untreated and MICP-treated soils microstructure. Fig. 16 shows the EDS image of the untreated sand. As can be seen from this figure, the sand structure is discontinuous and granular. Moreover, no bonds are visible between the sand grains.

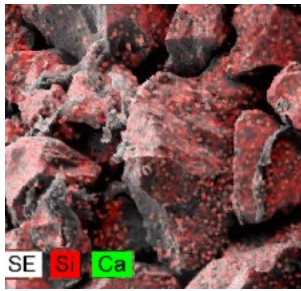


**Fig. 16.** Energy-dispersive X-ray spectroscopy (EDS) image of Kuhin sand

Fig. 17-18 show the SEM and EDS images of MICP-treated sand with 4 injection frequencies after curing days. The formed precipitated calcite between the sand particles is clearly visible in Fig. 18. The structure of the sand changed because of the development of precipitated calcite crystals between the sand particles. Comparison of Figures 16 and 18 illustrates great change in the soil structure. It is obvious that the structure of the untreated soil has changed from a grain based form in Fig. 16 to a more aggregated structure in figure 18, because  $\text{CaCO}_3$  can deposit at particle contacts, coat particles, and grow into the pore space. Fig. 19 shows the detected elements in EDS image for 4 injection MICP-treated sample.

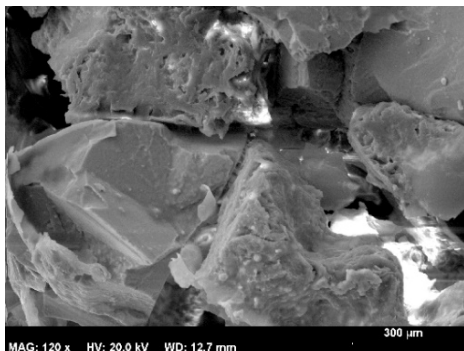


**Fig. 17.** Scanning electron microscopy (SEM) image of MICP-treated Kuhin sand

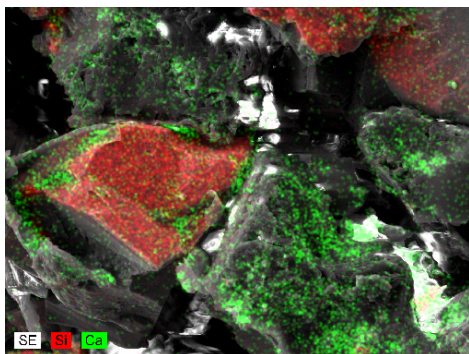


**Fig. 18.** EDS image of MICP-treated Kuhin sand and formed precipitated calcite

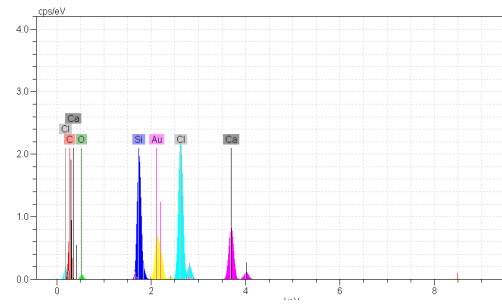


**Fig. 19.** Detected elements in EDS image for 4 injection MICP-treated sample

## 5. Summary and conclusions

In this study, the effect of microbially induced calcite precipitation (MICP)-treatment on the cyclic behavior of Kuhin sand was investigated. The most important results of the tests can be summarized as following cases:

Soil treatment with MICP had a significant effect on decreasing the potential of liquefaction. For example, the number of cycles causing liquefaction is changed from 6 for the untreated sand to 127 for the MICP-treated sample with 6 injection frequencies at 100kPa confining pressure and CSR of 0.2. This effect was owing to the cementation of precipitated calcite and hence binding of the soil particles.

Untreated sand exhibited a sudden growth in axial strain and reached a DAAS of 5% (liquefaction criterion) in fewer cycles (6 cycles); however, for the MICP-treated sand, increase in axial strain against applied cyclic loading is low at the beginning cycles and occurred gradually at the last cycles. When the number of loading cycles increases and the axial strain exceeds about 0.5%, the effect of precipitated calcite decreases and the axial strain amplitude starts to increase in a larger ratio almost the same as the untreated one.

Excess PWP in the MICP-treated sand increased gradually and more cycle is needed to reach the initial liquefaction, and also the initial liquefaction state didn't coincide with the failure.

MICP-treated samples demonstrated an inelastic behavior and the mean slope of the loops decreased from cycle to cycle, which is indicating stiffness degradation of these samples over cyclic loading.

The soil shear modulus increased due to MICP-treatment up to 67%. MICP-treatment leads to aggregation of soil structure and binding the soil particles. As an outcome of this phenomenon, particle deformation is decreased and thus the shear stiffness of the soil is increased.

The shear modulus of MICP-treated sand has increased with increasing confining pressure. Because the created bonds (due to calcite

precipitation) between the sand particles are supported by the confining pressure.

Due to the MICP-treatment, the damping ratio of the soil increased up to 50%. MICP-treatment, reduced soil deformations, but these reduced deformations almost occur as large-strains and lead to increase of damping ratio.

The SEM and EDS images of MICP-treated sand showed that the structure of the untreated sand has changed from a grain-based form to a more aggregated structure.

## References

- ASTM, "Standard Practice for Classification of Soils for Engineering Purposes (Unified Soil Classification System)", ASTM-D2487-17e1, 2017.
- ASTM, "Standard test methods for the determination of the modulus and damping properties of soils using the cyclic triaxial apparatus", ASTM-D3999, 2011.
- ASTM, "Standard Test Method for Particle-Size Analysis of Soils", ASTM-D422-63e2, 2007.
- ASTM, "Standard Test Methods for Maximum Index Density and Unit Weight of Soils Using a Vibratory Table", ASTM-D4253-16e1, 2016.
- ASTM, "Standard Test Methods for Minimum Index Density and Unit Weight of Soils and Calculation of Relative Density", ASTM-D4254-16, 2016.
- ASTM, "Standard test method for load controlled cyclic triaxial strength of the soil", ASTM-D5311, 2013.
- ASTM, "Standard Test Methods for Specific Gravity of Soil Solids by Water Pycnometer", ASTM-D854-14, 2014.
- Athukorala R, "Geotechnical characteristics of an erodible soil stabilised by lignosulfonate an analytical perspective", Ph.D dissertation, University of Wollongong, Wollongong, Australia, 2013.
- Banerjee A, Patil, UD, Puppala AJ, Hoyos LR, "Evaluation of Liquefaction Resistance in Silty Sand via Suction Controlled Cyclic Triaxial Tests", In PanAm Unsaturated Soils 2017, 2018, 543-552.  
<https://doi.org/10.1061/9780784481684.055>.
- Chen Q, Indraratna B, Rujikiatkamjorn C, "Behaviour of lignosulfonate-treated soil under cyclic loading", Proceedings of the Institution of Civil Engineers-Ground Improvement, 2016, 169 (2), 109-119.  
<http://doi.org/10.1680/grim.15.00004>.
- Darby KM, Hernandez GL, DeJong JT, Boulanger RW, Gomez MG, Wilson DW, "Centrifuge model testing of liquefaction mitigation via microbially induced calcite precipitation", Journal of Geotechnical and Geoenvironmental Engineering, 2019, 145 (10), 04019084-04019084.  
[http://doi.org/10.1061/\(ASCE\)GT.1943-5606.0002122](http://doi.org/10.1061/(ASCE)GT.1943-5606.0002122).
- DeJong JT, Fritzges MB, Nüsslein K, "Microbially induced cementation to control sand response to undrained shear", Journal of Geotechnical and Geoenvironmental Engineering, 2006, 132 (11), 1381-1392.  
[http://doi.org/10.1061/\(ASCE\)1090-0241\(2006\)132:11\(1381\)](http://doi.org/10.1061/(ASCE)1090-0241(2006)132:11(1381)).
- DeJong JT, Mortensen BM, Martinez BC, Nelson DC, "Bio-mediated soil improvement", Ecological Engineering, 2010, 36 (2), 197-210.  
<https://doi.org/10.1016/j.ecoleng.2008.12.029>.
- Fahoum K, Aggour MS, Amini F, "Dynamic properties of cohesive soils treated with lime", Journal of Geotechnical Engineering, 1996, 122 (5), 382-389.  
[https://doi.org/10.1061/\(ASCE\)0733-9410\(1996\)122:5\(382\)](https://doi.org/10.1061/(ASCE)0733-9410(1996)122:5(382)).
- Feng K, Montoya BM, "Influence of confinement and cementation level on the behavior of microbial-induced calcite precipitated sands under monotonic drained loading", Journal of Geotechnical and Geoenvironmental Engineering, 2016, 142 (1), 04015057.  
[https://doi.org/10.1061/\(ASCE\)GT.1943-5606.0001379](https://doi.org/10.1061/(ASCE)GT.1943-5606.0001379).
- Festugato L, Venson GI, Consoli NC, "Parameters controlling cyclic behaviour of cement-treated sand", Transportation Geotechnics, 2021, 27, 100488.  
<https://doi.org/10.1016/j.trgeo.2020.100488>.
- Guo L, Wang J, Cai Y, Liu H, Gao, Y, Sun H, "Undrained deformation behavior of saturated soft clay under long-term cyclic loading", Soil Dynamics and Earthquake Engineering, 2013, 50, 28-37.  
<https://doi.org/10.1016/j.soildyn.2013.01.029>.
- Han Z, Cheng X, Ma Q, "An experimental study on dynamic response for MICP strengthening liquefiable sands", Earthquake Engineering and Engineering Vibration, 2016, 15 (4), 673-679.  
<https://doi.org/10.1007/s11803-016-0357-6>.
- Harkes MP, Van Paassen LA, Booster JL, Whiffin VS, Van Loosdrecht MC, "Fixation and distribution of bacterial activity in sand to induce carbonate precipitation for ground reinforcement", Ecological Engineering, 2010, 36 (2), 112-117.  
<https://doi.org/10.1016/j.ecoleng.2009.01.004>.
- Hoyos LR, Puppala AJ, Chainuwat P, "Dynamic properties of chemically stabilized sulfate rich clay". Journal of Geotechnical and Geoenvironmental Engineering, 2004, 130 (2), 153-162.  
[https://doi.org/10.1061/\(ASCE\)1090-0241\(2004\)130:2\(153\)](https://doi.org/10.1061/(ASCE)1090-0241(2004)130:2(153)).
- Ismail MA, Joer HA, Randolph MF, "Sample preparation technique for artificially cemented soils", ASTM, Geotechnical Testing Journal, 2000, 171-177.  
<https://doi.org/10.1520/GTJ11041J>.
- Keramatikerman M, Chegenizadeh A, Nikraz H, "Experimental study on effect of fly ash on liquefaction resistance of sand", Soil Dynamics and Earthquake Engineering, 2017, 93, 1-6.  
<https://doi.org/10.1016/j.soildyn.2016.11.012>.
- Kokusho T, "Cyclic triaxial test of dynamic soil properties for wide strain range", Soils and foundations, 1980, 20 (2), 45-60.  
[https://doi.org/10.3208/sandf1972.20.2\\_45](https://doi.org/10.3208/sandf1972.20.2_45).
- Lin H, Suleiman MT, Brown DG, "Investigation of pore-scale CaCO<sub>3</sub> distributions and their effects on stiffness and permeability of sands treated by microbially induced carbonate precipitation (MICP)", Soils and Foundations, 2020, 60 (4), 944-961.  
<https://doi.org/10.1016/j.sandf.2020.07.003>.
- Lin H, Suleiman MT, Brown DG, Kavazanjian JrE, "Mechanical behavior of sands treated by microbially

- induced carbonate precipitation", *Journal of Geotechnical and Geoenvironmental Engineering*, 2016, 142 (2), 04015066.  
[https://doi.org/10.1061/\(ASCE\)GT.1943-5606.0001383](https://doi.org/10.1061/(ASCE)GT.1943-5606.0001383).
- Noorzad R, Amini PF, "Liquefaction resistance of Babolsar sand reinforced with randomly distributed fibers under cyclic loading", *Soil Dynamics and Earthquake Engineering*, 2014, 66, 281-292.  
<https://doi.org/10.1016/j.soildyn.2014.07.011>.
- Ozdogan A, "A study on the triaxial shear behavior and microstructure of biologically treated sand specimens", PhD thesis, University of Delaware, USA, 2010.
- Poulos HG, "Marine geotechnics", Unwin Hyman, Ltd, 1988, 90-149.
- Simatupang M, Okamura M, Hayashi K, Yasuhara H, "Small-strain shear modulus and liquefaction resistance of sand with carbonate precipitation", *Soil Dynamics and Earthquake Engineering*, 2018, 115, 710-718.  
<https://doi.org/10.1016/j.soildyn.2018.09.027>
- Ta'negonbadi B, Noorzad R, "Physical and geotechnical long-term properties of lignosulfonate-stabilized clay: An experimental investigation", *Transportation Geotechnics*, 2018, 17, 41-50.  
<https://doi.org/10.1016/j.trgeo.2018.09.001>.
- Van Paassen LA, Daza CM, Staal M, Sorokin DY, Van der Zon W, Van Loosdrecht MC, "Potential soil reinforcement by biological denitrification", *Ecological Engineering*, 2010, 36 (2), 168-75.  
<https://doi.org/10.1016/j.ecoleng.2009.03.026>.
- Van Paassen LA, "Biogrout, ground improvement by microbial induced carbonate precipitation", PhD thesis, TU Delft, Delft University of Technology, Netherlands, 2009.
- Wang M, Kong L, Zhao C, Zang M, "Dynamic characteristics of lime-treated expansive soil under cyclic loading", *Journal of Rock Mechanics and Geotechnical Engineering*, 2012, 4 (4), 352-359.  
<https://doi.org/10.3724/SP.J.1235.2012.00352>.
- Whiffin VS, "Microbial CaCO<sub>3</sub> precipitation for the production of biocement", Doctoral Dissertation, Murdoch University, Australia, 2004.
- Whiffin VS, Van Paassen, LA, Harkes MP, "Microbial carbonate precipitation as a soil improvement technique", *Geomicrobiology Journal*, 2007, 24 (5), 417-423.  
<https://doi.org/10.1080/01490450701436505>.
- Zhang X, Chen Y, Liu H, Zhang Z, Ding X, "Performance evaluation of a MICP-treated calcareous sandy foundation using shake table tests", *Soil Dynamics and Earthquake Engineering*, 2020, 129, 105959.  
<https://doi.org/10.1007/s11709-022-0865-6>.